Detection Sensitivity of Input Impedance to Local Defects in Long Cables

WENXIA PAN[1]**, XINRUI LI**[1]**, ZHENGDING ZHU**[2]**, KUN ZHAO**[1]**, (Student Member, IEEE), CHEN XIE**[1]**, AND QI SU**[3]**, (Senior Member, IEEE)**

[1]College of Energy and Electrical Engineering, Hohai University, Nanjing 210098, China
[2]State Grid Pinghu Electric Power Co., Ltd., Pinghu 314200, China
[3]Centre for Electrical Power Engineering, Monash University at Clayton, Clayton, VIC 3800, Australia

Corresponding author: Xinrui Li (mili0306@vip.qq.com)

ABSTRACT Broadband impedance spectroscopy (BIS) has become a new method for detecting cable insulation defects, but the sensitivity of this method to local defects in cables has not been fully studied. Taking long submarine cable as an example, firstly, the intrinsic correlations between the impedance spectroscopy characteristics and the cable parameters are studied, and the influence of local defects on the peak of impedance spectrum is studied by establishing a simplified model of long cables with insulation defects. Secondly, the formula for calculating the sensitivity of input impedance to the insulation defects is proposed and the characteristics of sensitivity are studied. Finally, the sensitivity of the input impedance to different positions and degrees of defects at the first resonant frequency is analyzed, which can be verified by simulation and experimental. The Results show that, for long cable with length l, under the condition of open-circuit, the sensitivity trends to zero when the defects occur at 25% or 75% of the cable length l, and under the condition of short-circuit, the sensitivity trends to zero when the defects occur to the end of the cable. Therefore, in the application of BIS, the above positions should be paid attention to, and the cable length can be changed and measured again to confirm its insulation status.

INDEX TERMS Submarine cable, distributed parameter circuits, cable insulation, broadband impedance spectroscopy (BIS), sensitivity, the resonant frequency.

I. INTRODUCTION

With the development of energy and the raise in electricity consumption, there is an increasing demand for trans-sea transmission. Cross-linked polyethylene (XLPE) submarine cable plays an important role in power transmission [1], [2]. In actual operation, submarine cables are exposed to high temperature environments for a long time, and their insulation layers are liable to be degraded. Failure to observe defects in time and take measures can easily lead to permanent failure of the cable and affect the safe and stable operation of the power system [3]. The research on cable insulation defect detection and location methods has certain foundation. Time Domain Reflectometry (TDR) is a widely used method [4], [5]. The basic idea of TDR method is to locate the defect by estimating the time difference between the incident and reflected pulse signals. However, the pulse signal will seriously decay when

it propagates in the cable, and the reflected wave formed at the defect is not obvious. Therefore, TDR cannot effectively identify the local defects of the cable, but is mainly used to locate the insulation fault. Another detection method is the Frequency Domain Reflectometry (FDR) developed from the perspective of the frequency domain. FDR uses frequency sweep signals to measure frequency parameters of cables, which solves the problem of low sensitivity of TDR to defects.

Broadband Impedance Spectroscopy (BIS) is a local defect localization method based on FDR [6]–[8]. The BIS method utilizes cable impedance measurements over a wide range of frequencies to obtain information on the dielectric properties. By developing algorithms, properties are extracted from these impedance measurements to characterize the condition of the cable. Because the cable input impedance spectrum can well represent the parameter characteristics at high frequencies, it provides a new direction for the research of local defect localization methods. Based on the principle

The associate editor coordinating the review of this manuscript and approving it for publication was Jenny Mahoney.

of BIS, the Halden Reactor Project developed the Line Resonance Analysis (LIRA) method for cable condition monitoring [9], [10]. This method extracts the characteristics of insulation defects by monitoring the line impedance and amplifying its phase and amplitude, but the related algorithms have not been published, and this method does not consider the frequency-varying effect of the cable distribution parameters at high frequencies. The research group of Yoshimichi Ohki in recent years imported the Inverse Fast Fourier Transform (IFFT) into analyzing the frequency domain spectra of the measured impedance magnitude or phase angle [11]–[14]. However, this method requires the measurement equipment to provide a very high frequency, which is difficult to achieve with existing equipment. Chinese scholars have proposed using the principle of generalized integration transformation (GIT) to select the kernel function of integral transformation, so as to construct insulation defects diagnostic function to realize the positions of insulation defects [15]. In addition, some scholars have proposed a precise location method based on the reflection coefficient spectrum, which can make up for the shortcomings of the broadband impedance spectrum method in locating the weak insulation defects of cables [16]. Although the above methods have made some achievements in the study of BIS, none of them had studied the intrinsic correlations between impedance spectroscopy and cable insulation defects and no research has pointed out the sensitivity of the impedance spectrum to insulation defects at different locations. The impedance spectroscopy is mainly suitable for the detection of insulation defects in short and medium cables, whether it is suitable for the case of long cable needs further research.

Therefore, in this paper, by establishing a simplified model of a long cable with insulation defects, the effect of local defects on the peak of the impedance spectrum is studied. The sensitivity formula of input impedance to local defects is proposed, and the sensitivity to different defect positions and levels at the first resonance frequency is studied, and verified by simulation and experiments.
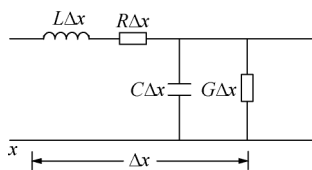

FIGURE 1. Equivalent circuit of the cable distributed parameters.

II. CABLE PARAMETERS AND IMPEDANCE SPECTROSCOPY

A. CABLE DISTRIBUTED PARAMETERS

According to the transmission line theory [17], under the condition of a high-frequency signal source, the submarine long cable can be represented by the distributed parameter model, which is shown in Fig. 1, resistance, R, inductance,

L, conductance, G, and capacitance, C are the distributed parameters of cable per-unit-length.

The effect on the distributed resistance at high frequencies is mainly the skin effect of the conductor, and the skin depth of the conductor δ decreases as the frequency increases, which is expressed as:

$$\delta(\omega) = \sqrt{\frac{2}{\omega \mu_0 \gamma_0}} \tag{1}$$

Here, ω is the angular frequency, μ_0 the permeability of the vacuum, and γ_0 the conductor conductivity.

In addition, there is a proximity effect between the coaxial cable core and the metal screen, so that the current concentrates on the conductor surface. The resistance R per-unit-length of these cables can be approximated by [18]:

$$R \approx \frac{1}{2\pi r_c \delta_c \gamma_c} + \frac{1}{2\pi r_s \delta_s \gamma_s} \tag{2}$$

Here, r_c and r_s are the core conductor radius and metal screen inner radius, γ_c and γ_s the corresponding conductivity.

The inductance of the coaxial cable includes the self-inductance of the inner and outer conductors and the mutual inductance between the two. The inductance L per-unit-length of these cables can be approximated by [18]:

$$L \approx \frac{\mu_0 \delta_c}{4\pi r_c} + \frac{\mu_0 \delta_s}{4\pi r_s} + \frac{\mu_0}{2\pi} \ln \frac{r_s}{r_c} \tag{3}$$

Equation (2) and (3) show that the resistance R increases with the square root of frequency, and inductance L decreases slightly with the increase of frequency [19]. The inductance L can be treated as a fixed value in the calculation. Both R and L are not sensitive to the cable insulation condition [20], which are almost unchanged if the cable insulation is defective.

The conductance G and capacitance C are related to permittivity and conductivity of insulation, which can be expressed by:

$$G = \frac{2\pi \sigma}{\ln(r_s / r_c)}$$
$$C = \frac{2\pi \varepsilon}{\ln(r_s / r_c)} \tag{4}$$

Here, ε and σ are the permittivity and conductivity of the insulating material, which vary with the insulation properties [21], so G and C are sensitive to the cable insulation condition.

B. CABLE IMPEDANCE SPECTROSCOPY

For a cable with a total length of l, the impedance measured at the beginning can be expressed as:

$$Z_{in} = Z_0 \frac{1 + \Gamma_L e^{-2\gamma l}}{1 - \Gamma_L e^{-2\gamma l}} \tag{5}$$

Here, Γ_L is the load reflection coefficient, which is given by:

$$\Gamma_L = \frac{Z_L - Z_0}{Z_L + Z_0} \tag{6}$$

where Z_L is load impedance, Z_0 is the characteristic impedance and γ is the propagation constant, which are given by (7).

$$\begin{cases} Z_0 = \sqrt{\dfrac{R + j\omega L}{G + j\omega C}} \\ \gamma = \alpha + j\beta = \sqrt{(R + j\omega L)(G + j\omega C)} \end{cases} \quad (7)$$

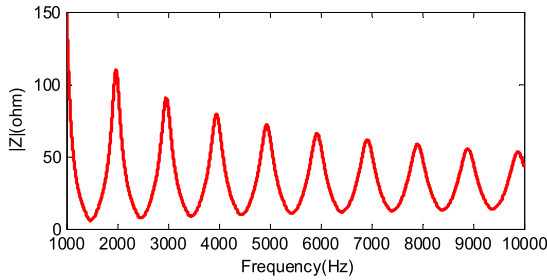where α is the attenuation constant, and β is the phase constant.

FIGURE 2. Impedance magnitude spectrum of 100 km long cable.

As an example, Fig. 2 shows the theoretical calculation of the impedance amplitude spectrum for a 100 km long cable. We observed that that the maximum and minimum values of the cable impedance magnitude spectrum appear periodically, and the values change quickly near the peaks of the impedance magnitude spectrum.

When $r = \Gamma_L e^{-2\alpha l}$, $\theta = 2\beta l$, the input impedance has the following form:

$$Z_{in} = Z_0 \frac{1 + r\cos\theta - jr\sin\theta}{1 - r\cos\theta + jr\sin\theta} \quad (8)$$

The magnitude of the input impedance is:

$$|Z_{in}| = |Z_0|\sqrt{\frac{1 + r^2 + 2r\cos\theta}{1 + r^2 - 2r\cos\theta}} \quad (9)$$

Equation (9) shows the relationship between the input impedance amplitude and the pulse frequency for a certain cable. At high frequencies, we considered $\omega L \gg R$, $\omega C \gg G$, so the characteristic impedance Z_0 can be regarded as the real number:

$$Z_0 \approx \sqrt{\frac{L}{C}} \quad (10)$$

Considering the different states of the cable end, under the condition of open-circuit, $r > 0$, and the input impedance magnitude reaches peaks when $\cos\theta = 1$, having the form:

$$|Z_{in}|_{\max} = |Z_0| \frac{1 + r}{1 - r} \quad (11)$$

At this time, $\theta = 2\pi k$ $(k = 1, 2, 3...)$, and because $\beta = \frac{2\pi f}{v}$, the frequencies at which the input impedance magnitude reaches peaks can be expressed as:

$$f_{|Z_{in}|\max} = \frac{k}{2l}\sqrt{\frac{1}{LC}} \quad (k = 1, 2, 3...) \quad (12)$$

Under the condition of short-circuit, $r < 0$, and the input impedance magnitude reaches peaks when $\cos\theta = -1$, the frequencies at which the input impedance magnitude reaches peaks can be expressed as:

$$f_{|Z_{in}|\max} = \frac{2k - 1}{4l}\sqrt{\frac{1}{LC}} \quad (k = 1, 2, 3...) \quad (13)$$

When the input impedance magnitude reaches the peaks, whether the cable is open-circuited or short-circuited, $e^{-2\gamma l}$ has the following form:

$$e^{-2\gamma l} = r \quad (14)$$

Therefore, $e^{-2\gamma l}$ is a real number. In the case of high frequencies, the characteristic impedance Z_0 is also regarded as a real number, so the input impedance Z_{in} can be regarded as resistance and $f_{|Z_{in}|\max}$ can be called the resonance frequency.

III. SENSITIVITY ANALYSIS OF INPUT IMPEDANCE TO INSULATION DEFECTS

A. CALCULATION MODEL OF INPUT IMPEDANCE WITH INSULATION DEFECTS

Because the change of the degree of insulation defect is mainly reflected in the change of the insulation resistance to ground [22], in order to facilitate the study of the sensitivity of the input impedance to the local defect, the resistance R_m is used to equivalent the local defect, and a model is established, as shown in Fig. 3. When the cable insulation defect deepens, the resistance R_m becomes smaller.
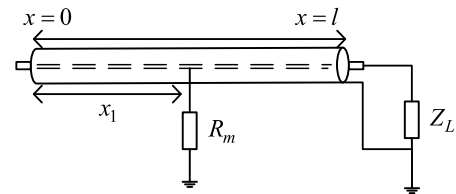

FIGURE 3. Cable with a local defect.

The input impedance from the defect position to the load is expressed as:

$$Z_{in1} = Z_0 \frac{1 + \Gamma_L e^{-2\gamma(l - x_1)}}{1 - \Gamma_L e^{-2\gamma(l - x_1)}} \quad (15)$$

where l is the length of cable, x_1 is the distance from the beginning of the cable to the defect. The resistance R_m representing the defect and the input impedance Z_{in1} from the defect position to the load can be equivalent to the load impedance Z_{load} at the defect:

$$Z_{load} = \frac{Z_{in1}R_m}{Z_{in1} + R_m} \quad (16)$$

The input impedance at the signal source $(x = 0)$ is computed by the following equation:

$$Z_{in} = Z_0 \frac{1 + \Gamma_1 e^{-2\gamma x_1}}{1 - \Gamma_1 e^{-2\gamma x_1}} \quad (17)$$

where the reflection coefficient Γ_1 at x_1 is given by:

$$\Gamma_1 = \frac{Z_{load} - Z_0}{Z_{load} + Z_0}$$
$$= \frac{2e^{-2\gamma(l-x_1)}R_m\Gamma_L - Z_0[1 + \Gamma_L e^{-2\gamma(l-x_1)}]}{2R_m + Z_0[1 + \Gamma_L e^{-2\gamma(l-x_1)}]} \quad (18)$$

The relationship between cable input impedance and insulation defects is revealed by (17) and (18).

B. INFLUENCE OF INSULATION DEFECTS ON INPUT IMPEDANCE SPECTRUM

According to the above analysis, the input impedance changes rapidly near the peaks of impedance magnitude spectrum, and the resonance points are sensitive to the changes in electrical parameters of the cable. Therefore, the next step is to study the effects of insulation defects on the peak of the input impedance magnitude spectrum.

Firstly, the case of insulation defects in the midpoint of the cable is taken as the research object, when the cable is open-circuit, the input impedance can be expressed as:

$$Z_{in} = Z_0\frac{2R_m(1+e^{-4\gamma x_1})+Z_0(1-e^{-4\gamma x_1})}{2R_m(1-e^{-4\gamma x_1})+Z_0(1+2e^{-2\gamma x_1}+e^{-4\gamma x_1})} \quad (19)$$

Taking a 220kV cable as an example, its length is 100 km, the cable core is copper, the outer diameter of the inner conductor is 40mm, and the insulating medium in the shielding layer is polyethylene.
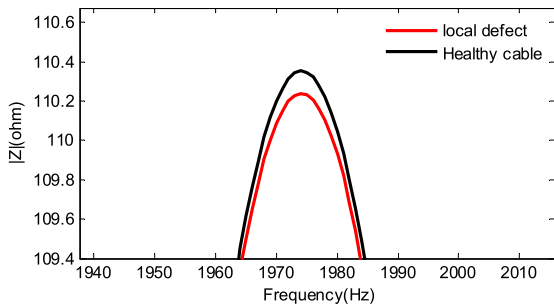
FIGURE 4. Enlarged comparison of cable input impedance magnitude spectrum.

Fig. 4 compares the peak of the impedance magnitude spectrum of the healthy and defective cable when R_m equals 0.1MΩ. According to (12), when the cable length is determined, the resonance frequency that makes the input impedance reach the peak depends on the distribution parameters of the cable. Because the local defect only changes the local distribution parameters of the cable, it has almost no effect on the overall distribution parameters [15]. so damaged cables and healthy cables have the same resonance frequency.

According to Fig. 4, when insulation defects occur in the cable, the magnitude of the input impedance decreases most near the peaks of the impedance spectrum. Therefore, this point can reflect the defects of the cable more sensitively. The impedance spectroscopy method developed a series of algorithms to extract characteristics from the first resonance point to detect the state of the cable.
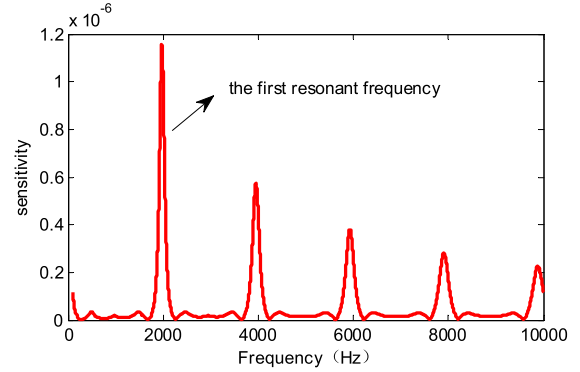
FIGURE 5. Sensitivity variation with frequency when the cable is open-circuited.

C. SENSITIVITY ANALYSIS

When $r = e^{-4\alpha x_1}$, $\theta = 4\beta x_1$, the input impedance of the opencircuited cable has the following form:

$$Z_{in} = Z_0[2R_m(1 + r\cos\theta) + Z_0(1 - r\cos\theta)]/n_p$$
$$+ jZ_0 r\sin\theta(Z_0 - 2R_m)/n_p \quad (20)$$

Here:

$$n_p = 2R_m(1 - r\cos\theta) + Z_0(1 + r\cos\theta + 2\sqrt{r}\cos\frac{\theta}{2})$$
$$+ jr(2R_m\sin\theta - Z_0\sin\theta - \frac{2Z_0}{\sqrt{r}}\sin\frac{\theta}{2}) \quad (21)$$

The magnitude of the input impedance is:

$$|Z_{in}| = |Z_0|\sqrt{\frac{m}{n}} \quad (22)$$

The sensitivity of input impedance to insulation defects is expressed by the partial derivative of the input impedance magnitude to resistance R_m:

$$\delta(R_m, f) = \frac{1}{2}|Z_0|(\frac{m}{n})^{-\frac{1}{2}}\frac{m'_{R_m}n - mn'_{R_m}}{n^2} \quad (23)$$

Here:

$$m = r^2(2R_m - Z_0)^2 + (8R_m^2 - 2Z_0^2)r\cos\theta + (2R_m + Z_0)^2$$
$$n = \sqrt{r}\cos\frac{\theta}{2}Z_0[8R_m(1 - r) + 4Z_0(1 + r)] + 4rZ_0^2$$
$$+ (2R_m - Z_0)^2r^2 + (2R_m + Z_0)^2 + 2r\cos\theta(Z_0^2 - 4R_m^2)$$
$$m'_{R_m} = 4r^2(2R_m - Z_0) + 4(2R_m + Z_0) + 16R_m r\cos\theta$$
$$n'_{R_m} = 8\sqrt{r}\cos\frac{\theta}{2}Z_0(1 - r) - 16rR_m\cos\theta$$
$$+ 4(2R_m - Z_0)r^2 + 4(2R_m + Z_0) \quad (24)$$

Take R_m as a fixed value, when $\cos\frac{\theta}{2} = 1$, $\theta = 4\pi k$ ($k = 1, 2, 3...$), the frequency is:

$$f_{|\delta|\max} = \frac{k}{l}\sqrt{\frac{1}{LC}} \quad (k = 1, 2, 3...) \quad (25)$$

When the cable is open-circuited, the resonant frequencies that make the sensitivity reaches its peaks is indicated by (25). Fig. 5 shows the sensitivity $\delta(R_m, f)$ varies with the frequency
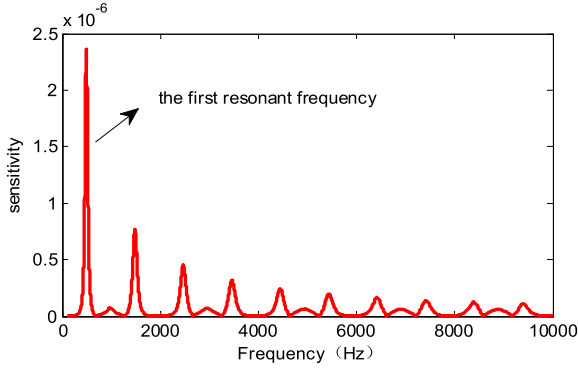
FIGURE 6. Sensitivity variation with frequency when the cable is short-circuited.

FIGURE 7. Sensitivity variation with R_m.
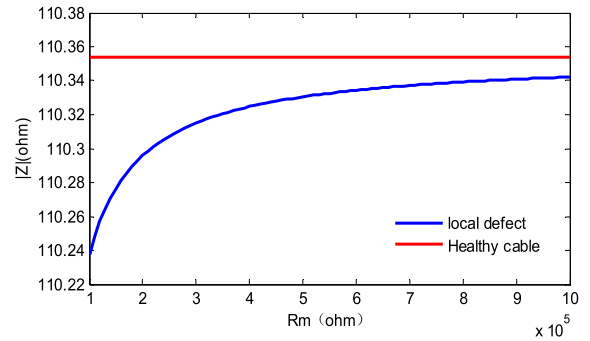
FIGURE 8. Input impedance magnitude variation with R_m.

when the insulation defect occurs to the midpoint of the open-circuited cable. Here, R_m was taken as $0.1M\Omega$, the frequency ranges from 100 Hz to 10 kHz. We observed that the sensitivity is the highest at the first resonant frequency 1974 Hz, and the peaks of sensitivity will decay with the increase of frequency. The first resonant frequency here is the frequency at which the input impedance magnitude reaches an initial peak.

When the cable is short-circuited, the sensitivity of the insulation defects is expressed as:

$$\delta(R_m, f) = \frac{1}{2}|Z_0|(\frac{n}{m})^{-\frac{1}{2}}\frac{n'_{R_m}m - nm'_{R_m}}{m^2} \tag{26}$$

Here:

$$
\begin{aligned}
m &= r^2(2R_m - Z_0)^2 + (2R_m + Z_0)^2 \\
&\quad + (8R_m^2 - 2Z_0^2)r\cos\theta \\
n &= (2R_m - Z_0)^2 r^2 + (2R_m + Z_0)^2 + 4rZ_0^2 \\
&\quad + \sqrt{r}\cos\frac{\theta}{2}Z_0[8R_m(r-1) - 4Z_0(1+r)] \\
&\quad + 2r\cos\theta(Z_0^2 - 4R_m^2) \\
m'_{R_m} &= 4r^2(2R_m - Z_0) + 4(2R_m + Z_0) + 16R_m r\cos\theta \\
n'_{R_m} &= 4(2R_m - Z_0)r^2 + 4(2R_m + Z_0) \\
&\quad + 8\sqrt{r}\cos\frac{\theta}{2}Z_0(r-1) - 16rR_m\cos\theta \tag{27}
\end{aligned}
$$

when $\delta(R_m, f)$ reaches peaks, the frequency is:

$$f_{|\delta|\max} = \frac{2k-1}{4l}\sqrt{\frac{1}{LC}} \quad (k = 1, 2, 3...) \tag{28}$$

When the cable is short-circuited, the resonant frequencies that make the sensitivity reaches its peaks is indicated by (28). Fig. 6 shows the sensitivity $\delta(R_m, f)$ varies with the frequency when the insulation defect occurs to the midpoint of the short-circuited cable. We observed that the first resonant frequency is 492 Hz.

Then the changes of sensitivity and input impedance at different degrees of defects are shown in Fig. 7 and 8 respectively under the condition of open-circuit. The frequency is 1974 Hz, and the resistance R_m ranges from $0.1M\Omega$ to $1M\Omega$.
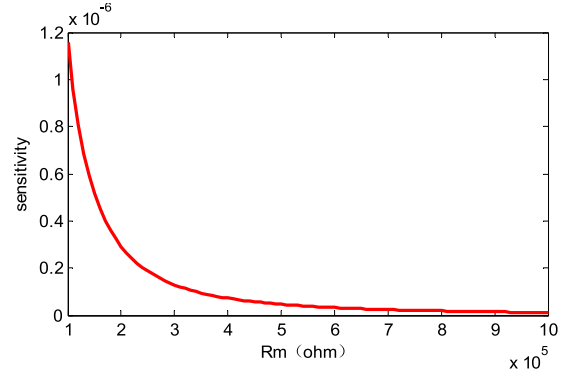
Fig. 7 and 8 show that the sensitivity becomes smaller and the impedance magnitude becomes larger as the R_m increases. Therefore, the sensitivity of input impedance to insulation defects is not only related to the frequency, but also to degrees of defects. The input impedance magnitude decreases slightly when the cable is slightly defective. As degrees of defects deepen, the sensitivity and the drop in the input impedance becomes lager.

IV. INFLUENCE OF DEFECTS POSITIONS ON SENSITIVITY

The above studies are all about the insulation defects at the midpoint of the cable. For the case of insulation defects in other positions, it is first necessary to determine the first resonant frequency.

When the insulation defect appears at x_1 from the cable head, since $R_m \gg Z_0$, $\frac{Z_0}{R_m} \to 0$, the input impedance formula can be simplified to:

$$
\begin{aligned}
Z_{in} &= Z_0\frac{2R_m(1+e^{-2\gamma l})+Z_0[1 + e^{-2\gamma(l-x_1)} - e^{-2\gamma x_1} - e^{-2\gamma l}]}{2R_m(1 - e^{-2\gamma l})+Z_0(1+e^{-2\gamma(l-x_1)}+e^{-2\gamma x_1}+e^{-2\gamma l}]} \\
&\approx Z_0\frac{1 + e^{-2\gamma l}}{1 - e^{-2\gamma l}} \tag{29}
\end{aligned}
$$

According to (29), the input impedance Z_{in} mainly depend on the propagation constant γ, and the propagation constant γ is only related to the frequency f for the determined cable, which means that the input impedance is only related to

the frequency, not to the defect position. Therefore, the first resonance frequency that makes the input impedance reaches the first peak is irrelevant to the defect position. When $r_p = e^{-2\alpha x_1}$, $\theta_p = 2\beta x_1$, the input impedance is:

$$Z_{in} = Z_0 \left\{ 2R_m(1+r) + Z_0[1+(\frac{r}{r_p}-r_p)\cos\theta_p - r] \right\} \Big/ m_p$$

$$+ jZ_0^2(\frac{r}{r_p}+r_p)\sin\theta_p \Big/ m_p \quad (30)$$

Here:

$$m_p = 2R_m(1-r) + Z_0[1+(\frac{r}{r_p}+r_p)\cos\theta_p + r]$$

$$+ jZ_0(\frac{r}{r_p}-r_p)\sin\theta_p \quad (31)$$

The sensitivity equation at different defect locations is:

$$\delta(R_m,f) = \frac{1}{2}|Z_0|(\frac{m_1}{n_1})^{-\frac{1}{2}} \frac{m'_{1R_m}n_1 - m_1 n'_{1R_m}}{n_1^2} \quad (32)$$

Here:

$$m_1 = [2R_m(1+r) + Z_0 + Z_0(\frac{r}{r_p}-r_p)\cos\theta_p - rZ_0]^2$$

$$+ Z_0^2(\frac{r}{r_p}+r_p)^2\sin^2\theta_p$$

$$n_1 = [2R_m(1-r) + Z_0 + Z_0(\frac{r}{r_p}+r_p)\cos\theta_p + rZ_0]^2$$

$$+ Z_0^2(\frac{r}{r_p}-r_p)^2\sin^2\theta_p$$

$$m'_{1R_m} = 4Z_0(1+r)[1+(\frac{r}{r_p}-r_p)\cos\theta_p - r] + 8R_m(1+r)^2$$

$$n'_{1R_m} = 4Z_0(1-r)[1+(\frac{r}{r_p}+r_p)\cos\theta_p + r] + 8R_m(1-r)^2$$

$$(33)$$

At the first resonance frequency, the resistance R_m is set to 0.1 MΩ, 0.2 MΩ and 0.5 MΩ, respectively, representing different defects. When the cable length is 100km, the sensitivity changes with the positions of the defects is shown in Fig. 9.
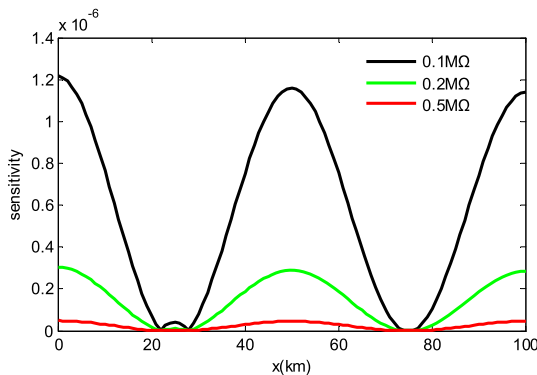
FIGURE 9. Sensitivity variation with the positions of defects when the 100km cable is open-circuited.

Fig. 9 shows that at the first resonant frequency 1974Hz, under the condition of open-circuit, the sensitivity is minimal
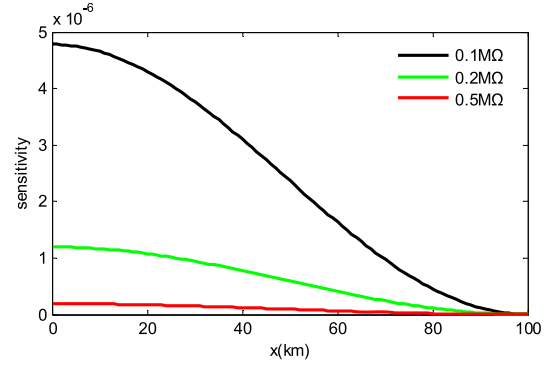
FIGURE 10. Sensitivity variation with the positions of defects when the 100km cable is short-circuited.

when defects occur at 25 km or 75 km, while the maximized sensitivity is about 1.2×10^{-6}.

When the cable is short-circuited, the sensitivity formula is found to be the same as open-circuit. when the frequency is 492 Hz, as shown in Fig. 10, the sensitivity is minimal when the defects occur to the end of the cable, while the maximal sensitivity is about 4.8×10^{-6}.

The above research is for the 100km cable. For comparison, the cable with a length of 80 km is also used to study the sensitivity. When the cable is open-circuited, the first resonant frequency is 2469Hz. When the cable is short-circuited, the first resonant frequency is 615Hz. The sensitivity changes with the positions of the defects is shown in Fig. 11 and Fig. 12.
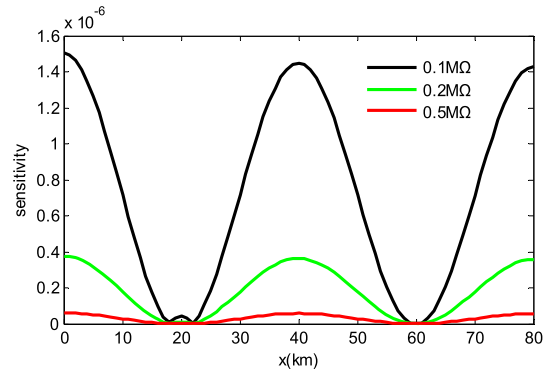
FIGURE 11. Sensitivity variation with the positions of defects when the 80km cable is open-circuited.

Under the condition of open-circuit, the sensitivity is minimal when the defects occur at 20 km or 60 km, while the maximal sensitivity is about 1.5×10^{-6}; under the condition of short-circuit, the sensitivity is minimal when the defects occur to the end of the cable, and the highest sensitivity is about 6×10^{-6}.

Based on the results of the 80km and 100km cables, the following conclusions can be drawn: under the condition of open-circuit, the sensitivity is minimal when the defects occur at 25% or 75% of the cable length *l*. under the condition
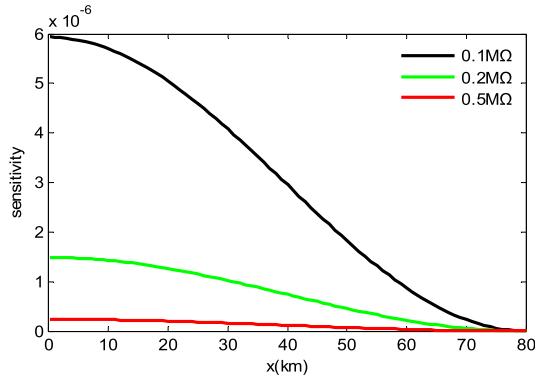
FIGURE 12. Sensitivity variation with the positions of defects when the 80km cable is short-circuited.

of short-circuit, the sensitivity is minimal when the defects occur to the end of the cable.

V. SIMULATION AND EXPERIMENTAL

In order to verify the theory of relationship between sensitivity and the degree and position of defects, the simulation and experimental verification are carried out respectively in this section. A 100 km cable model is established in the PSCAD, the core and the outer conductor are copper, the resistivity is $1.75 \times 10^{-8} \Omega \cdot m$, and the power source is 10 V. The outer diameter of the core is 40 mm, the inner diameter of the outer conductor is 80 mm, the insulating medium is polyethylene, and the relative permittivity is 2.3 [23].

Due to conditions, it is not possible to do experiments on long cables, so we use π section equivalent circuits to simulate the cable. As shown in Fig. 13, the 100 km cable consists of 20π section equivalent circuits.
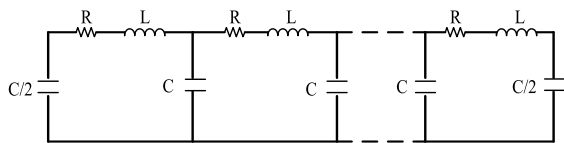

FIGURE 13. Equivalent model of experimental cable.

TABLE 1. Electrical parameters of each 5km cable.

$R_1(\Omega)$	$R_2(\Omega)$	$L_1(\text{H})$	$C_1(\text{F})$
0.697	0.348	6.9315×10^{-4}	9.226×10^{-7}
$R_3(\Omega)$	$R_4(\Omega)$	$L_2(\text{H})$	$C_2(\text{F})$
0.66	0.33	6.8×10^{-4}	1×10^{-6}

Because of the skin effect, the cable resistance is greatly affected by the difference in resonance frequency of open-circuit and short-circuit of cable. Table 1 shows the electrical parameters of each 5km cable. R_1, R_2, L_1 and C_1 are theoretical calculations, R_3, R_4, L_2 and C_2 are the component values used in the experimental, where R_1 and R_3 are open-circuit
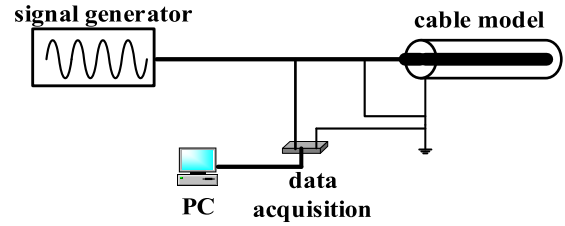

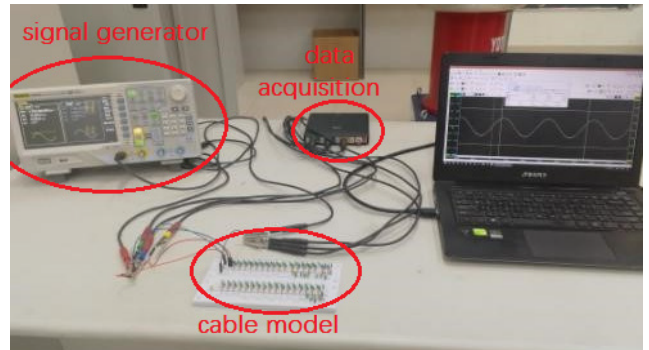**FIGURE 14. Schematic diagram of input impedance measurement.**

FIGURE 15. Experimental measurement platform.

resistance values, R_2 and R_4 are short-circuit resistance values.

The measurement principle is shown in Fig. 14 and the experimental measurement platform is shown in Fig. 15. The signal generator giving a 10V AC signal is connected to the beginning of the cable model, the voltage of the first π equivalent circuit resistance is measured through a data acquisition board, then the input current can be obtained according to the voltage on the resistance, finally the input impedance is calculated according to the input voltage and input current at the beginning. Slowly increase the frequency and record the frequency at which the input impedance reaches the first peak, i.e. the first resonant frequency.

Insulation defects are indicated by the grounding resistance of 0.1 MΩ, 0.2 MΩ and 0.5 MΩ, different resistance values indicate different degrees of defects. When the defects occur to x = 25 km, x = 50 km, x = 75 km and both ends of the cable, the input impedance was measured separately. The results are shown in Fig. 16 and 17.

The simulation results show that the first resonant frequencies of the open-circuit and short-circuit are 1918 Hz and 477 Hz, the input impedance of the healthy cable is 113.07 Ω and 213.19 Ω; the experimental results show that the first resonant frequencies of the open-circuit and short-circuit are 1916 Hz and 489 Hz. The input impedance of the healthy cable is 109.84 Ω and 201.61 Ω, respectively, measured in two cases.

The simulation and experimental results have the same trend, and the values differ by less than 5%. Therefore, the following conclusions can be drawn from Fig. 16 and 17: at the first resonant frequency, under the condition of open-circuit, the input impedance changes most when the defects occur
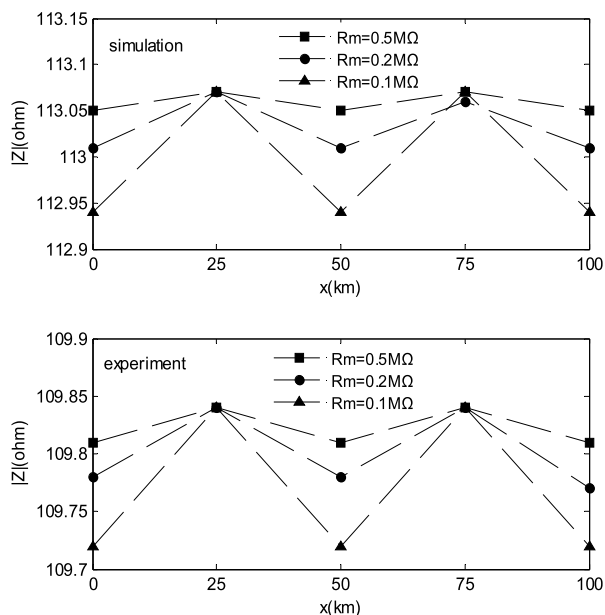
FIGURE 16. Input impedance magnitude variation with the positions of defects when the cable is open-circuited.
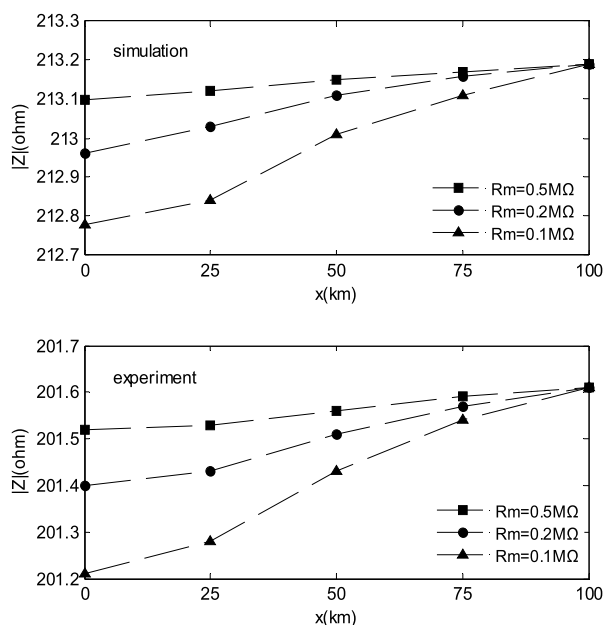

FIGURE 17. Input impedance magnitude variation with the positions of defects when the cable is short-circuited.

at the leading, end or the midpoint of the cable. The input impedance is almost constant when the defects occur to 25 km and 75 km. Under the condition of short-circuit, the input impedance changes the most when the defects occur to the beginning of the cable, while it changes minimally when the defects occur to the end. For the cable with different degrees of defects occurring at the same positions, the more serious the defects, the greater the change in the input impedance. Through experiments and simulations, the conclusions of the theoretical part are verified.

VI. CONCLUSION

Based on the principle of BIS to detect and locate local defects, this paper proposes to use sensitivity to characterize the effect of input impedance on reflecting defects. Finally, the sensitivities at different defect levels and positions was calculated. Results show that, for long cable with length l, under the condition of open-circuit, the sensitivity is minimal when the defects occur at 25% or 75% of the cable length l. Under the condition of short-circuit, the sensitivity is minimal when the defects occur to the end of the cable. The conclusion is verified by simulation and experiment. In actual application, in order to prevent the problem of insensitive detection when the defect occurs at the above position, the measurement can be repeated after artificially changing the cable length to effectively detect the entire cable.

REFERENCES

[1] T. Worzyk, *Submarine Power Cables: Design, Installation, Repair, Environmental Aspects*. Springer, 2009.

[2] W. Pan, K. Zhao, C. Xie, X. Li, J. Chen, and L. Hu, "Distributed online monitoring method and application of cable partial discharge based on φ-OTDR," *IEEE Access*, vol. 7, pp. 144444–144450, 2019.

[3] P. K. Ramteke, A. K. Ahirwar, N. B. Shrestha, V. V. S. S. Rao, K. K. Vaze, and A. K. Ghosh, "Thermal ageing predictions of polymeric insulation cables from Arrhenius plot using short-term test values," in *Proc. 2nd Int. Conf. Rel., Saf. Hazard-Risk-Based Technol. Phys.-Failure Methods*, Dec. 2010, pp. 325–328.

[4] E. Song, Y.-J. Shin, P. E. Stone, J. Wang, T.-S. Choe, J.-G. Yook, and J. B. Park, "Detection and location of multiple wiring faults via time–frequency-domain reflectometry," *IEEE Trans. Electromagn. Compat.*, vol. 51, no. 1, pp. 131–138, Feb. 2009.

[5] H. Lu, J. Qin, X. Chen, and B. Liu, "Overview of power cable fault location," (in Chinese), *Power Syst. Technol.*, vol. 28, no. 20, pp. 58–63, Oct. 2004.

[6] D. Rogovin and R. Lofaro, "Evaluation of the broadband impedance spectroscopy prognostic/diagnostic technique for electric cables used in nuclear power plants," Division Fuel, Eng., Radiol. Res., Office Nucl. Regulatory Res., US Nucl. Regulatory Commission, Rockville, MD, USA, Tech. Rep. NUREG/CR-6904, 2006.

[7] Y. Ohki, T. Yamada, and N. Hirai, "Diagnosis of cable aging by broadband impedance spectroscopy," in *Proc. Annu. Rep. Conf. Elect. Insul. Dielectric Phenomena*, Cancún, Mexico, Oct. 2011, pp. 24–27.

[8] N. Hirai, T. Yamada, and Y. Ohki, "Comparison of broadband impedance spectroscopy and time domain reflectometry for locating cable degradation," in *Proc. IEEE Int. Conf. Condition Monitor. Diagnosis*, Bali, Indonesia, Sep. 2012, pp. 229–232.

[9] P. F. Fantoni, "Wire system aging assessment and condition monitoring: The line resonance analysis method (LIRA)," Inst. Energy, Halden, Norway, Tech. Rep. HWR–788, 2005.

[10] P. F. Fantoni and A. Nordlund, "Wire system aging assessment and condition monitoring (WASCO)," Nordic Nuclear Safety Research, Nord. Kernsikk, Tech. Rep. NKS-130, 2006.

[11] Y. Ohki and N. Hirai, "Location feasibility of degradation in cable through Fourier transform analysis of broadband impedance spectra," *IEEJ Trans. Fund. Mat.*, vol. 132, no. 2, pp. 122–128, 2012.

[12] N. Hirai and Y. Ohki, "Highly sensitive detection of distorted points in a cable by frequency domain reflectometry," in *Proc. Int. Symp. Electr. Insulating Mater.*, Jun. 2014, pp. 144–147.

[13] T. Yamada, N. Hirai, and Y. Ohki, "Improvement in sensitivity of broadband impedance spectroscopy for locating degradation in cable insulation by ascending the measurement frequency," in *Proc. IEEE Int. Conf. Condition Monitor. Diagnosis*, Bali, Indonesia, Sep. 2012, pp. 677–680.

[14] Y. Ohki and N. Hirai, "Effects of the structure and insulation material of a cable on the ability of a location method by FDR," *IEEE Trans. Dielectrics Electr. Insul.*, vol. 23, no. 1, pp. 77–84, Feb. 2016.

[15] Z. Zhou, D. Zhang, J. He, and M. Li, "Local degradation diagnosis for cable insulation based on broadband impedance spectroscopy," *IEEE Trans. Dielectrics Electr. Insul.*, vol. 22, no. 4, pp. 2097–2107, Aug. 2015.

[16] M. Xie, "A new location method of local defects in power cables based on reflection coefficient spectrum," (in Chinese), *Power Syst. Technol.*, vol. 41, no. 9, pp. 3083–3089, 2017.

[17] L. N. Dworsky, *Modern Transmission Line Theory and Applications*. New York, NY, USA: Wiley, 1979.

[18] P. Van der Wielen, "On-line detection and location of partial discharges in medium voltage cables," Ph.D. dissertation, Dept. Elect. Power, Eindhoven Univ., Eindhoven, The Netherlands, 2005.

[19] B. S. Guru and H. R. Hiziroglu, *Electromagnetic Field Theory Fundamentals*. Cambridge, U.K.: Cambridge Univ. Press, 2009.

[20] J. Densley, "Ageing mechanisms and diagnostics for power cables— An overview," *IEEE Elect. Insul. Mag.*, vol. 17, no. 1, pp. 14–22, Jan. 2001.

[21] P. Werelius, P. Tharning, R. Eriksson, B. Holmgren, and U. Gafvert, "Dielectric spectroscopy for diagnosis of water tree deterioration in XLPE cables," *IEEE Trans. Dielectrics Electr. Insul.*, vol. 8, no. 1, pp. 27–42, Mar. 2001.

[22] X. Wei, B. Zhu, B. Pang, S. Wang, and R. Li, "On-line insulation monitoring method for long distance three-phase power cable," *Proc. CSEE*, vol. 35, no. 8, pp. 2079–2086, Apr. 2015.

[23] M. Liu, W. Pan, Y. Zhang, K. Zhao, S. Zhang, and T. Liu, "A dynamic equivalent model for DFIG-based wind farms," *IEEE Access*, vol. 7, pp. 74931–74940, 2019.

KUN ZHAO (Student Member, IEEE) received the B.S. degree in electrical engineering, in 2017. He is currently pursuing the M.S. degree in electrical engineering with Hohai University, Nanjing, China. His main research interests include wind power generation technology, and high voltage and insulation technology.

WENXIA PAN received the B.S. and M.S. degrees from Wuhan University, Wuhan, China, in 1982 and 1987, respectively, and the Ph.D. degree from Hohai University, Nanjing, China, in 2004. She is currently a Professor of electrical engineering with Hohai University. She has published two research books and authored or coauthored over 100 journal articles. Her current research interests include renewable energy generation systems, and high voltage and insulation technology.

CHEN XIE received the B.S. degree in electrical engineering, in 2017. He is currently pursuing the M.S. degree in electrical engineering with Hohai University, Nanjing, China. His main research interests include wind power generation technology and high voltage and insulation technology.

XINRUI LI received the B.S. degree in electrical engineering, in 2016. She is currently pursuing the M.S. degree in electrical engineering with Hohai University, Nanjing, China. Her main research interests include wind power generation technology, and high voltage and insulation technology.

ZHENGDING ZHU received the B.S. and M.S. degrees from Hohai University, Nanjing, China, in 2014 and 2019, respectively. His main research interests include high voltage and insulation technology, especially power cable technology, and power transmission technology.

QI SU (Senior Member, IEEE) received the M.Eng. degree in electrical engineering from the Wuhan University of Hydraulic and Electric Engineering, Wuhan, China, in 1981, and the Ph.D. degree in high-voltage engineering from the University of New South Wales (UNSW), Sydney, Australia, in 1990. He is currently a Guest Professor with Monash University, Melbourne, Australia. He holds two Australian patents and has published over 150 journal articles and conference papers. He has written two books, entitled *Condition Assessment of High Voltage Insulation in Power System Equipment* published by IET Press, in 2008, and *Electromagnetic Transients in Transformer and Rotating Machine Windings* published by ISI Global, USA, in 2012. His main research interests include insulation condition monitoring, reliability-centered maintenance, fuzzy diagnosis of electrical plant and transformers, and generator high-frequency models. He was a Fellow of IET.

● ● ●